TITLE:

Neoepitope formation through the generation of RNA-derived "editopes"

AUTHORS

Beatrice Casati[1,2,6], Veronica Pinamonti[2,3,4,6], Riccardo Pecori[1,5,6], John M. Lindner[3], Fotini Nina Papavasiliou[1,*]

[1]Division of Immune Diversity, Department of Immunology and Cancer, German Cancer Research Centre (DKFZ), 69120 Heidelberg, Germany.

[2]Faculty of Biosciences, Heidelberg University, 69120 Heidelberg, Germany.

[3]BioMed X Institute, 69120 Heidelberg, Germany.

[4]Current affiliation: Department of Experimental Oncology, European Institute of Oncology IRCCS, Milan, Italy.

[5]Helmholtz Institute for Translational Oncology (HI-TRON), Mainz, Germany.

[6]These authors contributed equally.

*Corresponding author.

KEYWORDS

ADAR, targeted RNA editing, cancer neoepitopes, MART-1, immunotherapy

ABSTRACT

Treatment-resistant tumors are frequently characterized by a low tumor mutational burden (TMB) and poor T-cell infiltration into the tumor microenvironment. Conversely, good responses to immunotherapy have been associated with high TMB and T-cell infiltration. This may imply that at least a subset of mutations in TMB-high tumors result in the generation of neoepitopes that are recognized (and cleared) by T cells. Currently, methods that specifically mutate MHC-presented tumor epitopes, while preserving genomic integrity, do not exist. Here, we have employed site-directed RNA editing to specifically alter MHC-presented tumor epitopes at the transcript level, with no modification to the genomic DNA, to modulate their antigenicity and recognition by cognate T-cell receptors (TCR). We demonstrate that RNA editing can be employed as a precision tool to specifically modulate antigenicity through the formation of RNA editing derived neoepitopes, which we have termed "editopes". In particular, we show potent induction of a T-cell response to an optimally edited peptide (40%) compared to a non-immunogenic mutant peptide (<2%) and its WT counterpart (20%). This study shows the potential of RNA editing as a method to improve tumor recognition by T cells and to favor tumor clearance.

INTRODUCTION

Immunotherapy has become a paradigm for the treatment of an increasing number of cancer types over the past two decades (1). However, a considerable number of patients do not respond to such

therapies (2). One factor associated with responsiveness to immunotherapy is a high TMB (3, 4), which has been suggested to lead to a high number of immunogenic cancer neoepitopes presented by the tumor cells. Moreover, it has recently been shown that not only genomic mutations can generate immunogenic cancer neoepitopes but also alternative splicing and RNA modifications (5), including RNA deamination, a modification that is also known as RNA editing (6).

RNA editing is a co- or post-transcriptional mechanism that introduces base changes to messenger RNA (7). In the animal kingdom, the majority of observed editing events is catalyzed by the Adenosine Deaminases Acting on RNA (ADAR) enzyme family (8). The catalytically active members of this family, ADAR1 and ADAR2, deaminate adenosine (A) into inosine (I) in double-stranded RNA molecules (dsRNAs) (9). RNA editing mediates specific functional outcomes depending on where it occurs on the transcript: coding region editing, although rare, can alter decoding and thus protein sequence (6, 10), while the far more common editing identified within non-coding regions can affect splicing, RNA stability, transcript localization, and translational efficiency, and thus overall protein levels within cells (11, 12).

Most RNA editing is mediated by ADAR1, a ubiquitous enzyme with specific roles in RNA sensing and innate defense against RNA viruses. Loss of ADAR1 leads to inflammation and cell death in most healthy tissues through the accumulation of unedited endogenous dsRNA and consequent activation of corresponding sensing pathways (13–16). Overexpression of ADAR1, on the other hand, is observed in most tumor tissues in comparison with their healthy counterparts, implying a role in maintaining tumor fitness through proteome diversification (17, 18).

Aside from its natural roles in health and disease, the ability of ADAR1 to target adenosines within dsRNA has been exploited for therapeutic purposes. Specifically, it was recognized almost three decades ago, and then repeatedly confirmed in the past decade, that through provision of an antisense guide RNA (gRNA) ADAR1 could be targeted to any transcript of interest (19–21). This recognition has led to a plethora of approaches (reviewed in (22)) that have been used to successfully correct point mutations at the RNA level and restore gene function (20, 21, 23–36).

Correction of gene defects requires sufficient editing efficiency to restore a functional phenotype, as well as high specificity in terms of negligible editing of neighboring bases (termed “bystander” editing) to avoid the generation of undesired mutations. However, the potential of introducing mutations has led us to envision a novel application of targeted RNA editing: here we apply site-directed RNA editing to introduce point mutations at the RNA level rather than correcting them. Specifically, by targeting ADAR to potentially immunogenic epitopes that are either not presented by tumor cells or not recognized by T cells in their genomically encoded state, we generate RNA editing-derived neoepitopes, which we call “editopes”. Since the abundance of mutations in tumors is strongly associated with positive responses to immunotherapy and longer patient survival (3), we propose that the targeted generation of such editopes at the RNA level will mimic a high tumor mutational burden and increase responsiveness to immunotherapy (37). As a first step towards this approach, we show that restoration (through editing) of a specific immunogenic epitope, MART-1$_{26\text{-}35}$ (Melanoma-Associated Antigen Recognized by T cells-1), can activate its cognate TCR DMF5 (38). These experiments provide proof of concept for the eventual therapeutic use of editopes in tumours with low mutation burden, that are currently non-responsive to checkpoint inhibitors.

RESULTS

Specific mutations within MART-1 ablate its recognition by the cognate TCR.

To assess the feasibility of using site-directed RNA editing to generate editopes, we designed a proof-of-concept experiment leveraging a well-studied system based on the MART-1 antigen (39). MART-1 is processed from the full-length *MLANA* transcript and presented by HLA-A2, for recognition by the DMF5 T-cell receptor, which is known to interact with the immunodominant high-affinity decameric MART-1$_{26\text{-}35}$ epitope (ELAGIGILTV) (**Figure 1a**) (40, 41). To generate a feasible target for site-directed RNA editing, we created a non-immunogenic variant of MART-1$_{26\text{-}35}$ via DNA mutagenesis by replacing a guanosine (G) with an adenosine (A) in the *MLANA* cDNA (DNA sequence GAGCTTGCTGGGATC**A**GCATCCTGACAGTG, with the mutated A highlighted in bold), which we could revert to the original sequence using targeted RNA

editing (**Figure 1a**). This G-to-A mutation induced an amino acid change at position 31 from glycine (G) into serine (S), resulting in the epitope sequence ELAGI**S**ILTV, where the mutated amino acid is highlighted in bold (**Figure 1a**). We then transduced HEK293T cells with a full-length *MLANA* cDNA expressing the WT or mutant peptide. These cells (the "tumor cells" in our experiment) should be recognized by a specific TCR (DMF5), which we generated by transducing an engineered TCR-deficient human cell line (Jurkat) with TCR alpha and beta chains encoding the DMF5 T-cell receptor (here referred to as DMF5 T cells or DMF5 Jurkat cells).

We then co-cultured "tumor" (MLANA-expressing HEK293T cells) and cognate T cells (Jurkat transduced with DMF5), and quantified functional responses by measuring T-cell surface expression of CD69, a proximal signal for T-cell activation. HEK293T-*MLANA* WT cells were able to activate DMF5 Jurkat cells with an average efficiency of approximately 20% (**Figures 1b** and **S1a**). In contrast, HEK293T cells transduced with the mutated *MLANA* construct showed an almost complete abrogation of T-cell activation, with fewer than 2% of the Jurkat cells expressing surface CD69 on average (**Figure 1b** and **S1a**). These results demonstrate that the *MLANA* G31S variant can be employed as an experimental model to test whether site-directed RNA editing can be used to generate functional neoepitopes.

Site-directed RNA editing restores the target mutation with high efficiency.

To edit the G31S MART-1 epitope and restore the WT version that would lead to T-cell activation, we used the established λN-ADAR site-directed editing system (21, 28, 42). Among the available targeted RNA editing systems, the λN-ADAR system is the smallest in size, and therefore the only one that can be encoded within lentiviral vectors, allowing us to create stable cell lines. λN-ADAR is known as a "two-component" system: it contains a specific guide RNA (gRNA) complementary to the target, flanked by sequences known as boxB loops (43), together with the deaminase domain of the hyperactive version of the editing enzyme ADAR2 ($ADAR2_{DD}^{E488Q}$) (44) fused to the λN phage protein. The natural interaction between the λN peptide and the boxB structures (43) allows the recruitment of the enzyme by the gRNA, which binds the target mRNA by complementarity. An A:C mismatch between the target and the gRNA favors efficient editing at the desired site (**Figure 1a** and (45)).

To generate the final lentiviral vector for our experiments, we modified the *MLANA*-expressing vector to carry all the components of the editing system. Specifically, we added the λN-ADAR and an OX40L-flag reporter under the same promoter of *MLANA* and the gRNA targeting the mutation in the *MLANA* transcript under the control of a U6 promoter (**Figure 2a**). Six copies of this latter cassette were inserted because this was previously shown to improve editing efficiency (31). We then transduced HEK293T cells and sorted for expression of the OX40L reporter indicating stable expression of the integrated construct. Following integration, the targeted transcript was reverse transcribed, PCR-amplified and the editing level was analyzed by Sanger sequencing. An on-target editing efficiency of 80% was observed across three biological replicates (**Figure 2b**). However, off-target editing events were also detected, most prominently at an adenosine 3 bases downstream of the target site (**Figure 2b**). As controls, cells expressing the target *MLANA* transcript and the editing enzyme without gRNAs were also included and did not show any edited sites along the targeted region, demonstrating that editing was indeed gRNA dependent (**Figure S2a**).

Since the off-target editing could ablate recognition of the epitope by the specific TCR (and subsequent T-cell activation), single transcripts were sequenced to detect whether on- and off- target editing events occurred on the same or different transcripts. We found that while most of the transcripts only carried the on-target editing, as expected, a minority of the transcripts showed on- and off- target editing at the same time (**Figure 2c**). This would be predicted to result in an editope with an undesirable amino acid change (I32V) (**Figure 2d**). We therefore checked whether the newly obtained editope was able to activate DMF5 T cells. We transduced HEK293T cells with a lentiviral vector expressing a mutated *MLANA* cDNA coding for the epitope carrying the unwanted I32V mutation (ELAGIG**V**LTV). Following co-culture with DMF5 T cells almost no T-cell activation was observed (**Figure 2e**) indicating that this off-target editing led to an editope unable to activate its cognate T cell clone.

An optimized editing system reduces off-target editing and improves editope recognition by cognate T cells.

To optimize the system, we therefore proceeded to implement a variety of methods that have been published by others to reduce off-target editing. We first fused a nuclear localization signal (NLS) to the λN-ADAR2$_{DD}^{E488Q}$, which was previously reported to reduce off-target editing (42, 46). A direct comparison of the editing level in the presence or absence of the NLS indeed showed a significant reduction in the editing frequency at the off-target site, while a similar on-target editing efficiency was maintained (**Figures 2b and 3a-b**). Therefore, we proceeded with the NLS-fused editing enzyme for all subsequent experiments. Further optimization of the system was attempted by optimizing the gRNA by introducing an A:G mismatch at the off-target site between the target (A) and the gRNA (G), which was previously reported to reduce off-target editing (47). The fully optimized editing system completely abolished off-target editing, resulting in a reproducible on-target editing of 90% (**Figure 3c**).

After confirming the editing efficiency, HEK293T cells expressing the optimized editing system and *MLANA* G31S were co-cultured with DMF5 Jurkat cells. Notably, the optimized editing system led to a T-cell activation of approximately 40% (**Figures 3d** and **S3**), indicating that the editope was indeed able to induce specific T-cell activation and even increase the level observed in the presence of the WT epitope.
To ensure that co-expression of the gRNAs with the target mRNA does not affect the expression of the latter, we introduced an additional control in which the WT *MLANA* mRNA was co-expressed with gRNAs complementary to the target except for the A:G mismatch at the recurrent off-target editing site. Interestingly, we observed a decrease in T-cell activation (**Figures S4a-b**). However, loss or downregulation of the integrated construct in the transduced and sorted HEK cells was excluded by confirming the expression of a reporter gene within the same expression cassette at the time of the T-cell activation assay (**Figure S4c**). Therefore, we checked for any off-target editing events despite the optimized gRNAs and we observed a new off-target editing site three bases upstream of the original target site (**Figure S4d**). This change induces a substitution of the fifth amino acid (isoleucine, I) by a glycine (G) resulting in yet another editope with the sequence ELAG**V**GILTV (with the mutated amino acid in bold) (**Figure S4e**), suggesting a cause for the reduced T-cell activation.

DISCUSSION

Cancer neoepitopes are mutation- or alternative-splicing-derived peptides that are presented on the surface of tumor cells, marking them as “foreign”. Such cells are the target of specific T cells within the tumor microenvironment. Activation of tumor specific T cells through the provision of specific antibodies that block inhibitory receptors on their surface can eliminate tumours both in preclinical models (48) and in the clinic, revolutionizing cancer treatment over the last decade. But only highly mutated tumors (which are presumably also those presenting the most neoepitopes) are actually amenable to treatment by T-cell activation. Indeed, a high tumor mutation burden (defined as 1 mutation in 10^5 nt) is a strong predictor of treatment responsiveness (3, 49). Still, the majority of tumors are not nearly as hypermutated, and therefore are not responsive to immunotherapy. Such tumors are termed mutationally “cold”; increasing their mutation burden is currently the focus of intense research.

Increasing the availability of neoepitopes within a tumor has been attempted both through “unsupervised” approaches (e.g. adjuvant radiation therapy to mutagenize tumor cells) or through more specific means, such as personalized cancer “vaccines” in the form of mRNAs expressing multiple peptide-linked neoepitopes, which aim to raise the number of cognate T-cell clonotypes (50). Here we propose another approach, which is to use targeted RNA editing to “mutate” neoepitopes at the level of RNA, thus creating “editopes”. We have illustrated the potential of this approach through a proof-of-concept experiment (**Figure 1a**). Specifically, we introduced a missense mutation to the known immunogenic MART-1$_{26-35}$ epitope, leading to loss of interaction with the cognate TCR on T cells (**Figure 1b**). We then successfully rescued the original sequence of the epitope (**Figure 3c**) via targeted RNA editing with the λN-ADAR system and recovered its ability to activate specific T cells (**Figure 3d**) (21, 28, 31, 42). Notably, after optimizing the RNA-editing system, we observed higher *in vitro* “immunogenicity” than when using the

wild-type *MLANA* sequence, suggesting that in addition to introducing desirable mutations, transcript targeting also increases the total levels of presented peptide.

Multiple studies have recently shown promising results in employing RNA editing to correct single point mutations, both in cells (19–21, 23, 24, 27–29, 31, 33–35, 42, 51–53) and in animal models (25, 26, 30, 32). These studies have revealed the following major weaknesses in the system: (a) editing can never reach 100% efficiency; (b) off-target (or bystander) editing is more of a problem than initially expected (though it can be ameliorated) (42, 46, 47). These are problematic weaknesses in the context of mutation correction but are indeed potentially beneficial to the approach we describe here, which aims not to correct, but rather to induce a mutation in RNA.

Therapeutically, editopes are meant to be generated using antisense oligos (ASOs) capable of recruiting endogenous ADAR, such as that achieved in previous studies (26, 27, 29, 30, 36). Ideally, a targeted delivery method to administer such editope-generating ASOs specifically to tumors will be beneficial, although even systemic administration is possible. This is because most cancer cells overexpress ADAR1 relative to the healthy tissue that surrounds them (17), affording a degree of selectivity toward the tumor. Indeed, the expression of ADAR1 and therefore its editing level is crucial for the functionality of RNA editing-derived neoepitopes, which are also presented on the surface of healthy cells but at such a low frequency that they do not trigger an immune response (6).

Practically, this system is not limited to one ASO and one editope – indeed, multiple ASOs can be used to generate several editopes within the same cell at the same time. In the context of cancer immunotherapy, a multi-editope approach would recruit a cohort of oligoclonal T cells to a tumor, thus circumventing immune evasion. This multi-targeted approach has been used by others in the context of personalized cancer vaccines (50). A recent study has already reported how such naturally occurring editopes (or RNA editing-derived cancer neoepitopes) can induce a specific antitumor immune response (6). In contrast to personalized cancer vaccines, the editope generating ASOs do not need to be tailored to individual patient “neoepitopes”. Instead, they only need to be tailored to individual cancer-entity-defining epitopes that will be converted into neoepitopes (or editopes) by targeted editing, which is a key advantage to other personalized approaches.

Overall, by demonstrating the potential of site-directed RNA editing as a strategy to modulate tumor immunogenicity, our study takes the first step toward a more ambitious goal: favoring tumor responsiveness to immunotherapy through editope formation.

FIGURES

Figure 1

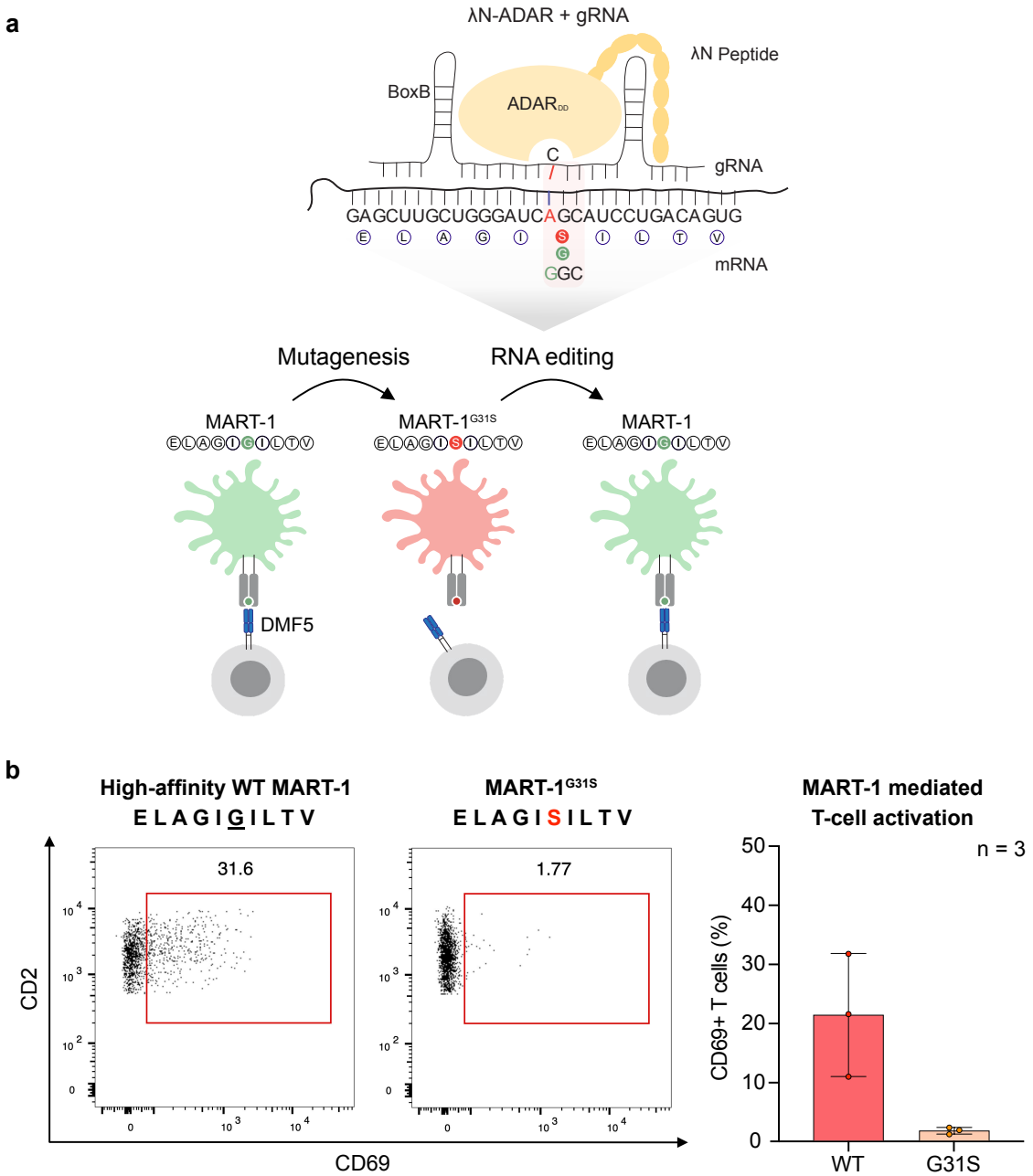

Figure 1. Experimental strategy and proof of principle demonstrating the feasibility of using RNA editing to boost tumor immunogenicity.
a. Schematic of the proof-of-principle experiment: the well-known tumor antigen, Melan-A, is genetically modified such that its processing results in a peptide (Melanoma antigen recognized by T-cells-1 or MART-1) no longer recognized by T cells. Targeted RNA editing is then applied to restore the original MART-1 sequence and thus rescue antigen-specific T-cell activation. The RNA and amino acid sequences of wild-type, mutated, and edited MART-1 are shown at the bottom. The modified bases and amino acids are highlighted in bold. **b.** Left: Representative dot plots showing CD69 expression (X axis) as a marker of

DMF5 T-cell activation when co-cultured with HEK293T cells expressing either high-affinity wild-type (WT) MART-1 or MART-1^{G31S}. The amino acid sequences of the WT and mutated peptides are shown above the respective dot plot, with the different amino acids underlined (WT) or highlighted in red (mutated). CD2 expression level is represented on the Y axis as a T-cell marker. Right: Bar plot showing the average T-cell activation across three biological replicates. The corresponding dot plots are shown in Figure S1a.

Figure 2

a

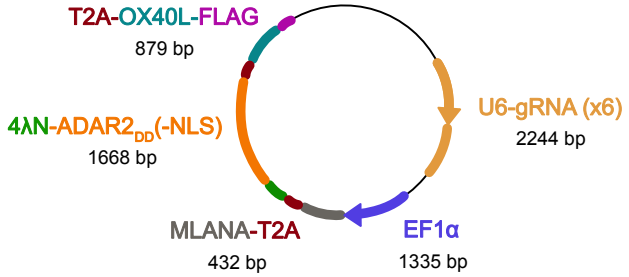

b

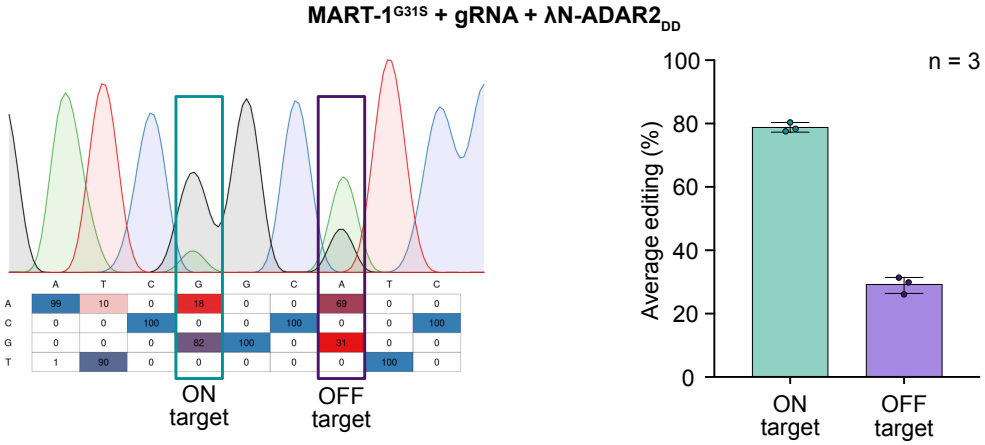

c

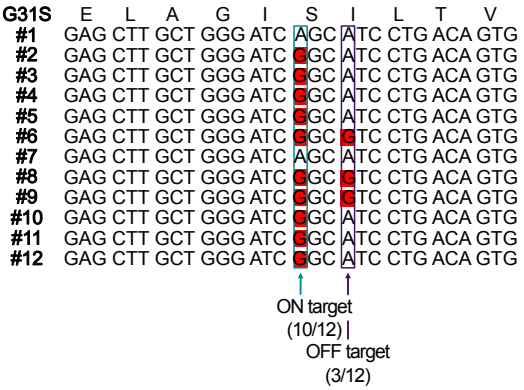

d

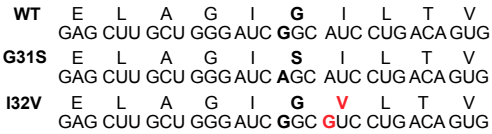

e

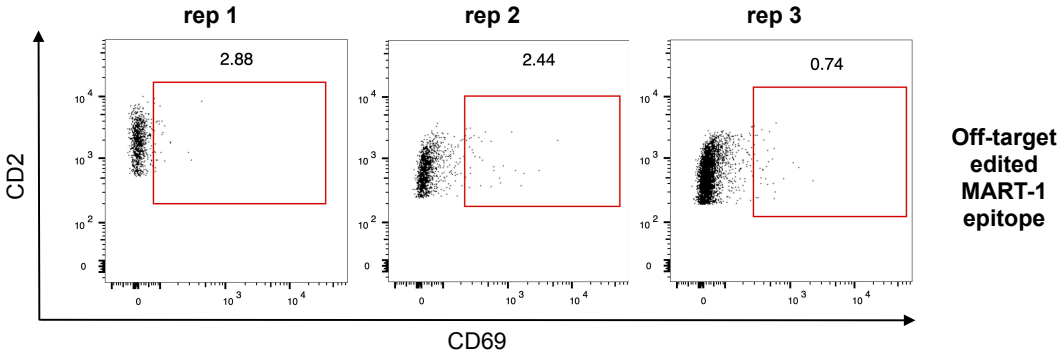

Figure 2. Site-directed RNA editing restores the target mutation with high efficiency.
a. Schematic of the lentiviral vector expressing the core components of the RNA editing system: six copies of the MLANA-targeting gRNA, each under control of the U6 promoter, *MLANA* cDNA (either wild-type or G31S, both high-affinity) under control of the EF1α promoter, followed by a T2A proteolytic cleavage site and a region coding for four copies of the λN peptide fused to the hyperactive ADAR2 catalytic domain ($ADAR2_{DD}^{E488Q}$) fused to the c-myc Nuclear Localization Signal (NLS), followed by T2A and the sequence coding for OX40L fused to a FLAG sequence as a reporter for successful lentiviral transduction. **b.** Left: Representative chromatogram of the edited region of the *MLANA* transcript. The on- and off-target sites are highlighted by a green and purple frame, respectively. Right: Bar plot showing the average editing level at the on- and off-target sites across three biological replicates. **c.** Multisequence alignment of the MART-1-coding region of the edited *MLANA* sequence upon ligation of amplicons in pJET1.2 vectors for single transcript sequencing analysis. The on- and off-target sites are highlighted by a green and purple frame, respectively. The bases highlighted in red indicate editing sites. **d.** RNA and amino acid sequences of wild-type (WT) MART-1, MART-1^{G31S} and off-target editing derived MART-1^{I32V}. The desired modifications at the RNA and protein levels are highlighted in black bold. The off-target editing derived modifications at the RNA and protein levels are highlighted in red bold. **e.** Dot plots showing CD69 expression (X axis) as a marker of T-cell activation of DMF5 T cells co-cultured with HEK293T cells expressing MART-1^{I32V}. CD2 expression level is represented on the Y axis as a T-cell marker.

Figure 3

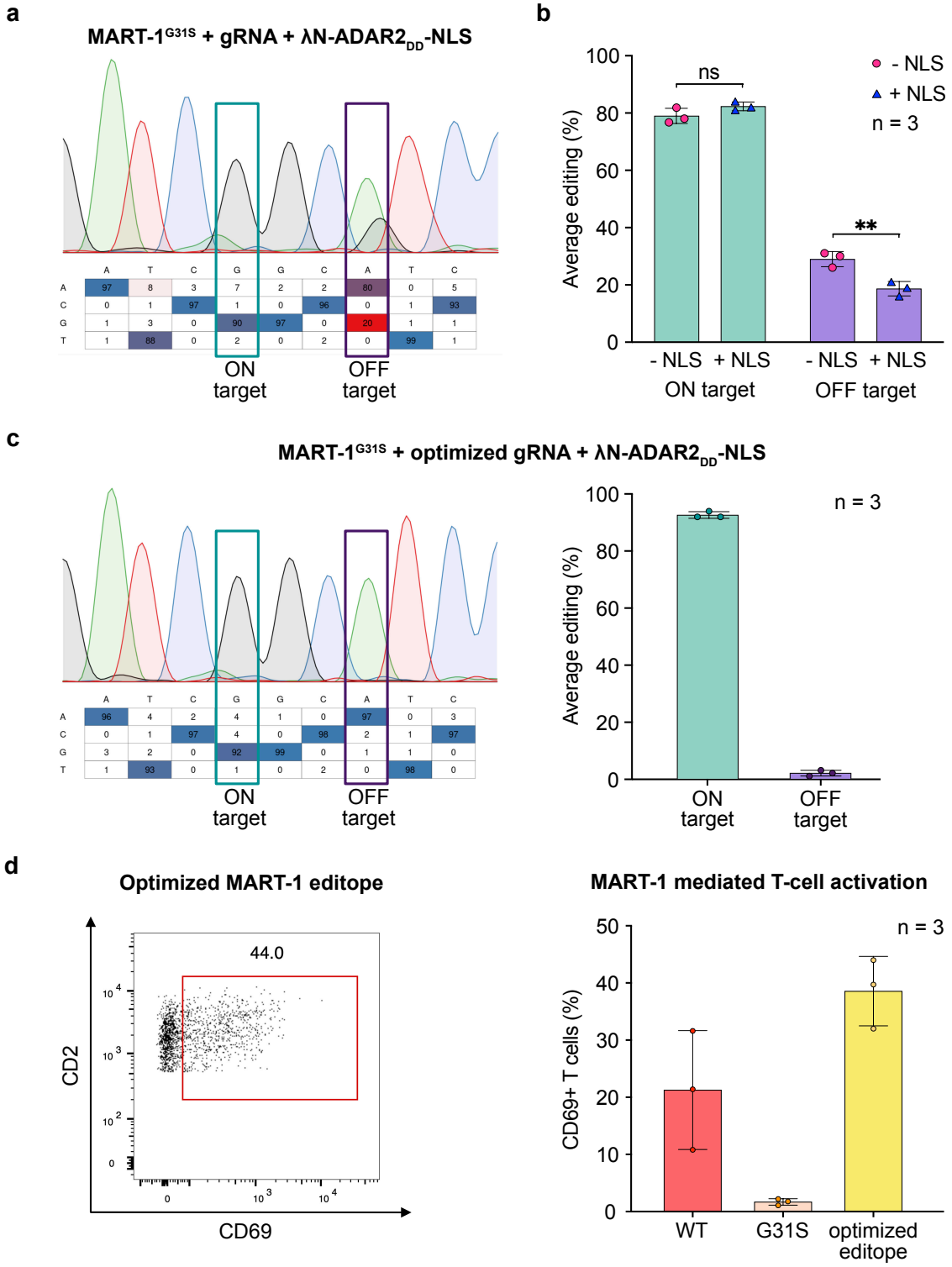

Figure 3. An optimized editing system reduces off-target editing and rescues the immunogenicity of a mutated epitope.

a. Representative chromatogram of the edited region of the *MLANA* transcript after fusing a nuclear localization signal (NLS) to the λN-ADAR2$_{DD}^{E488Q}$. The on- and off-target sites are highlighted by a green and purple frame, respectively. **b.** Bar plot showing the average editing level at the on- (green) and off- (purple) target sites achieved with λN-ADAR2$_{DD}^{E488Q}$ fused (pink) or not (blue) with a nuclear localisation signal (NLS) across 3 biological replicates. Representative chromatograms of the targeted region of the *MLANA* transcript edited by λN-ADAR2$_{DD}^{E488Q}$ fused or not with a NLS are shown in Figures 2b and 3a, respectively. ** P = 0.0080; ns = not significant; t-test, unpaired and two-tailed. **c.** Left: Representative chromatogram of the targeted region of the *MLANA* transcript upon inducing editing with the optimized gRNA. The on- and off-target sites are highlighted by a green and purple frame, respectively. Right: Bar plot showing the average editing level with the optimized gRNA at the on- and off-target sites across three biological replicates. **d.** Left: Representative dot plot showing CD69 expression (X axis) as a marker of T-cell activation of DMF5 T cells co-cultured with HEK293T cells expressing MART-1^{G31S} after inducing editing with the optimized gRNA. CD2 expression level is represented on the Y axis as a T-cell marker. Right: Bar plot showing the average T-cell activation across three biological replicates. The corresponding dot plots are shown in Figure S3.

SUPPLEMENTARY FIGURES

Supplementary figure 1

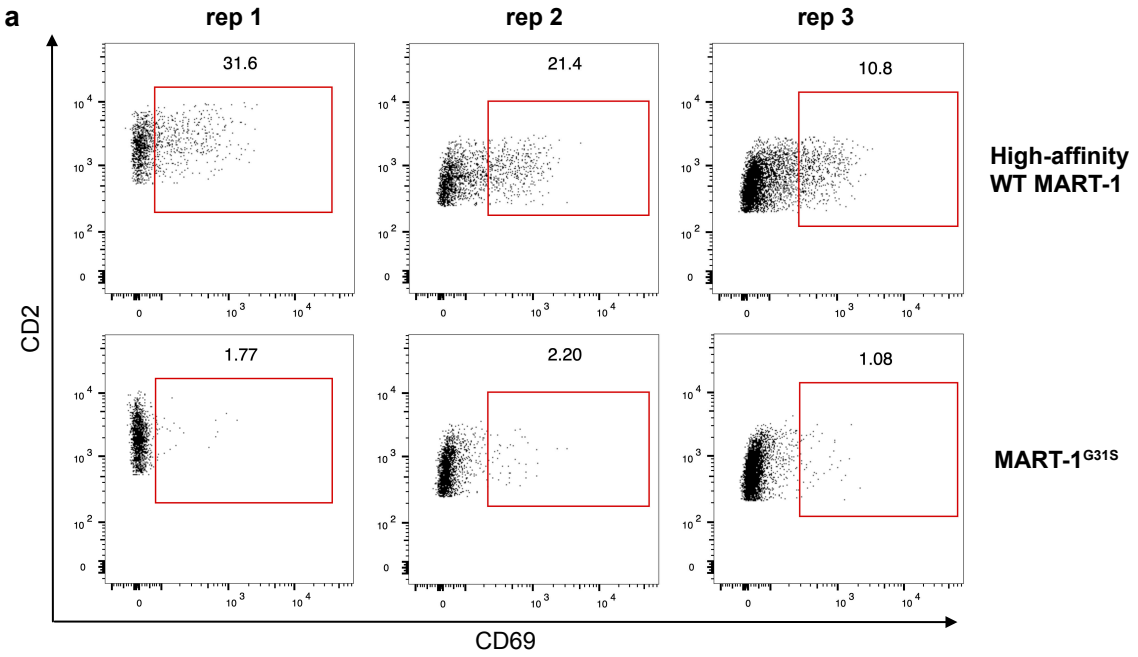

Figure S1: RNA editing rescues the immunogenicity of a mutated epitope.
a. Dot plots showing CD69 expression (X axis) as a marker of T-cell activation of MART-1 specific T cells co-cultured with HEK293T cells expressing either high-affinity wild-type (WT) or MART-1^{G31S} across three biological replicates. CD2 expression level is represented on the Y axis as a T-cell marker. One representative replicate is shown in Figure 1b.

Supplementary figure 2

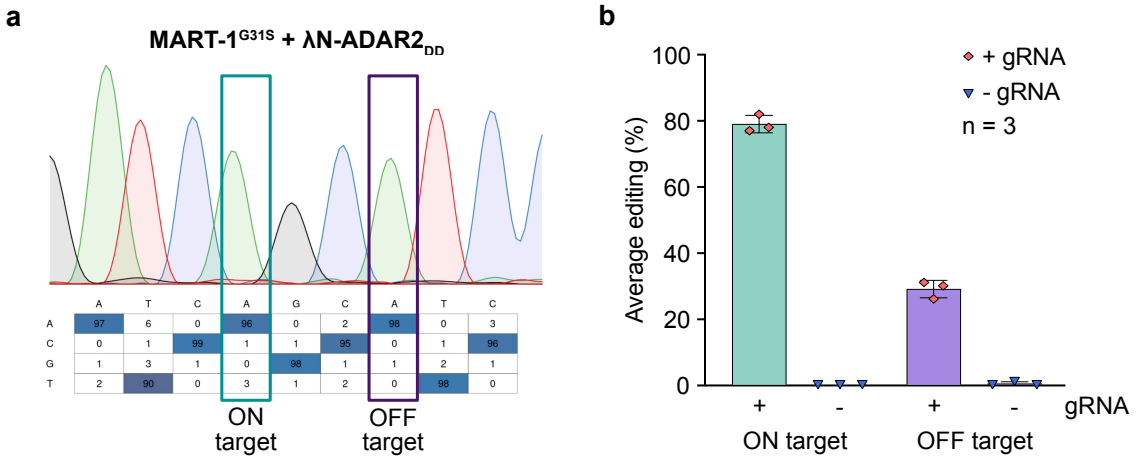

Figure S2: RNA editing rescues the immunogenicity of a mutated epitope.

a. Representative chromatogram of the targeted region of the *MLANA* transcript in cells expressing MART-1^{G31S} and λN-ADAR2$_{DD}^{E488Q}$ without gRNAs. The on- and off-target sites are highlighted by a green and purple frame, respectively. **b.** Bar plot showing the average editing level at the on- (green) and off- (purple) target sites of the targeted region of the *MLANA* transcript obtained in cells expressing MART-1^{G31S} and λN-ADAR2$_{DD}^{E488Q}$ with (coral red diamonds, "+") or without (blue triangles, "-") gRNAs across 3 biological replicates. Representative chromatograms of the targeted region of the *MLANA* transcript edited by λN-ADAR2$_{DD}^{E488Q}$ with or without gRNAs are shown in Figures 2b and S2a, respectively.

Supplementary figure 3

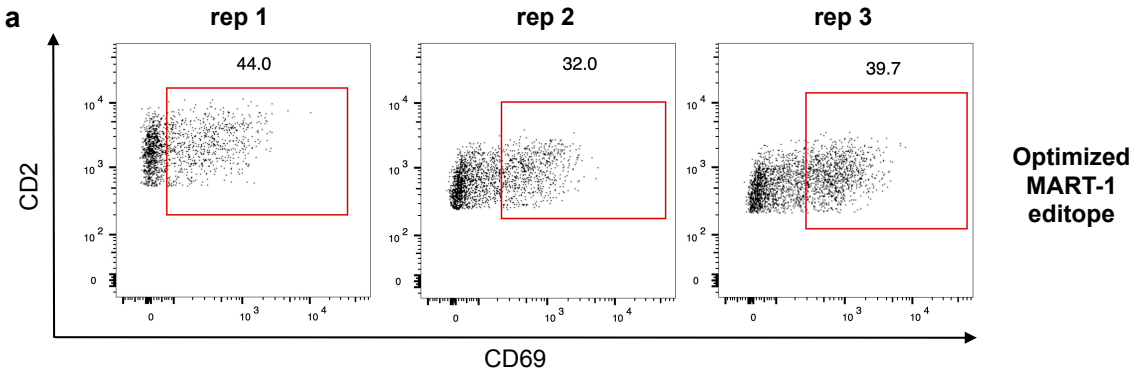

Figure S3: An optimized editing system reduces off-target editing and improves the editope immunogenicity.

a. Dot plots showing CD69 expression (X axis) as a marker of T-cell activation of DMF5 T cells co-cultured with HEK293T cells expressing MART-1^{G31S} after inducing editing with the optimized editing system across three biological replicates. CD2 expression level is represented on the Y axis as a T-cell marker. One representative replicate is shown in Figure 3d.

Supplementary figure 4

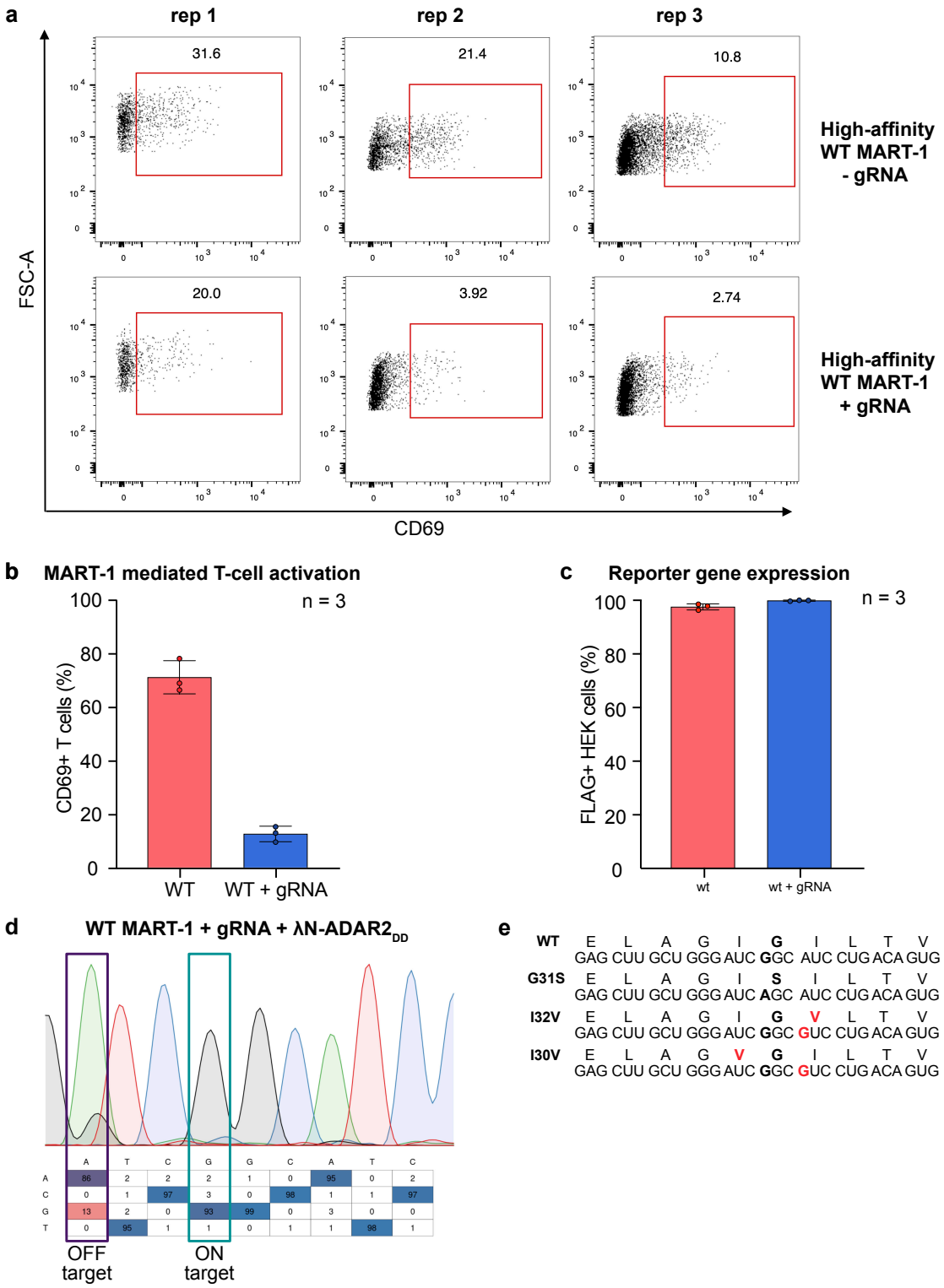

Figure S4: Low levels of off-target editing can affect downstream T-cell activation.

a. Dot plots showing CD69 expression (X axis) as a marker of T-cell activation of MART-1 specific T cells co-cultured with HEK293T cells expressing the high-affinity wild-type (WT) MART-1 with or without gRNA across three biological replicates. CD2 expression level is represented on the Y axis as a T-cell marker. **b**. Bar plot showing the average T-cell activation of MART-1 specific T cells co-cultured with HEK293T cells expressing the high-affinity wild-type (WT) MART-1 with or without gRNA across three biological replicates. **c**. Bar plot showing the average reporter gene expression in MART-1 specific T cells co-cultured with HEK293T cells expressing the high-affinity wild-type (WT) MART-1 with or without gRNA across three biological replicates. **d**. Representative chromatogram of the targeted region of the *MLANA* transcript in cells expressing WT MART-1 and λN-ADAR2$_{DD}^{E488Q}$ with gRNAs complementary to the MART-1 coding region of the *MLANA* transcript apart from an A-to-G mismatch at the site where off-target editing was recurrently observed in this study. The on- and novel off-target sites are highlighted by a green and purple frame, respectively. **e**. RNA and amino acid sequences of wild-type (WT) MART-1, MART-1^{G31S} and off-target editing derived MART-1^{I32V} and MART-1^{I30V}. The desired modifications at the RNA and protein levels are highlighted in black bold. The off-target editing derived modifications at the RNA and protein levels are highlighted in red bold.

METHODS

Cell culture

HEK293T cells were cultured in DMEM (Thermo Fisher Scientific GmbH 61965059) with 10% FBS and 1% penicillin-streptomycin (Capricorn Scientific PS-B) at 37°C in a humidified 5% CO_2 atmosphere. TCR-deficient Jurkat cells were cultured in RPMI 1640 Medium + 10% heat-inactivated (56°C for 20 min) FBS and 1% penicillin-streptomycin at 37°C in a humidified 5% CO_2 atmosphere. Jurkat cells expressing DMF5 TCR were cultured with 1 µg/ml Puromycin (Invivogen ant-pr-1).

Lentiviral production and transduction

HEK293T cells were used for lentiviral production; the day before transfection 3 x 10^5 cells were plated in 6 well plates in 2 ml of medium. For each transfection 0.67 µg of PMD2.G, 1 µg of PAX2 lentiviral transfer plasmids together with 1.3 µg of plasmid were used. DNA was mixed in 200 µl of Optimem (Gibco 31985062) before adding 6 µl of TransIT VirusGen Transfection Reagents (VWR International GmbHMIRUMIR6700). The transfection mixture was incubated for 10 to 15 min and then added dropwise on HEK293FT cells. 48h after transfection, viral supernatant was collected and sterile filtered with a 0.45 µm syringe filter (Th. Geyer GmbH & Co. KG 16537K). For the transduction, 7 µg/ml polybrene Polybrene (Thermo Fisher Scientific GmbH 11360039) was added to each viral sample. After 24h, cells were washed, and the medium was replaced with a fresh one without additives.

Cell sorting

Five days after transduction, 3 x 10^6 HEK293T cells were prepared for cell sorting to select cells with the desired construct integrated. Samples were diluted in FACS buffer (PBS with 2mM EDTA and 2% FBS) and centrifuged at 300 g for 5 min. The supernatant was removed, and cells were washed another time before the staining. Staining was performed using 50 µl of FACS buffer containing the anti-FLAG antibody diluted 1:200. Samples were incubated at 4°C for 20 minutes; samples were washed twice and resuspended in a final volume of 500 µl of FACS buffer. Positive cells were sorted using Fusion I Richard Sweet (BD Biosciences) and collected in 1.5 ml tubes, before being transferred to a suitable cell culture plate depending on the number of recovered cells.

Co-culture experiment and flow cytometry analysis

2.5 x 10^4 HEK293T cells were plated in a 96-well flat bottom plate. 24h later 1 x 10^5 T cells were plated on top in a total volume of 75 µl. The experiment was incubated for 16h in the incubator before FACS staining. Samples were diluted in FACS buffer (PBS with 2mM EDTA and 2% FBS) and centrifuged at 300 g for 5 min. The supernatant was removed, and cells were washed another time before the staining. Staining was performed using 50 µl of FACS buffer containing the antibodies diluted 1:200. Samples were incubated at

4°C for 20 minutes; samples were washed twice and resuspended in a final volume of 100 µl of FACS buffer. Samples measurements were recorded using FACS Aria II (BD Biosciences), and data were analyzed with FlowJo.

RNA extraction

Within 24 hours from the co-culture setup, RNA was extracted from 1 x 10^6 transduced HEK293T cells with the RNeasy Plus Mini Kit (Qiagen, #74134) following the manufacturer's instructions. RNA was quantified by Nanodrop (NanoDrop One, Thermo Scientific).

RT-PCR and Sanger sequencing

RT-PCR was performed on the extracted RNA with One-Step RT-PCR kit (Qiagen, #210212) according to the manufacturer's instructions and the following conditions. 500 ng of RNA was added to 14 µl of RNase-free water, 5 µl of 5x One-Step RT-PCR Buffer, 1 µl of dNTP mix (10 mM each), 1.5 µl of each primer (10 µM) and 1 µl of One-Step RT-PCR enzyme mix in a final reaction volume of 25 µl. *MLANA* amplification was obtained with the forward primer 5' - ATGCCCAGGGAGGACGCCCA - 3' and the reverse primer 5' - ACCGGGGCTGTATGGTGGAG - 3'. The RT-PCR program was run as follows: retrotranscription at 50°C for 30 min, denaturation at 95°C for 15 min, followed by 35 cycles of denaturation at 94°C for 30 sec, annealing at 69°C for 30 sec and elongation at 72°C for 40 sec. In the end a final elongation step at 72°C was run for 10 min. The correct size of the RT-PCR products (357 bp) was checked on a 1.5% agarose gel. PCR clean-up was performed on the correct RT-PCR products according to the manufacturer's instructions (Macherey-Nagel, #740609.250). 4-6 ng of each product were sent for Sanger sequencing to Eurofins Genomics Germany GmbH.

Editing analysis

The sequenced samples were analyzed for editing efficiency with the online available software MultiEditR (46).

Lentiviral vector design

The plasmid used for lentiviral transduction is depicted in Figure 2a. It contains *MLANA* cDNA coding for high-affinity MART-1_{26-35} either in its wild-type (ELAGIGILTV) or mutated (ELAGISILTV) form under control of the EF1α promoter, followed by a T2A proteolytic cleavage site and a region coding for four copies of the λN peptide fused to the hyperactive ADAR2 catalytic domain ($ADAR2_{DD}^{E488Q}$) fused to the c-myc Nuclear Localization Signal (NLS), followed by T2A and the sequence coding for OX40L fused to a FLAG sequence as a reporter for successful lentiviral transduction. The *MLANA* cDNA and the λN-$ADAR2_{DD}$(-NLS) sequence were first amplified by Q5 High Fidelity PCR from plasmids expressing each region separately. The lentiviral vector was then opened with the restriction enzymes EcoRI-HF (NEB, #R3101) and BamHI-HF (NEB, R3136) to cut out the region between these sites. Here, the PCR products were then inserted into the opened vector with NEBuilder (NEB, #E5520). Six copies of the *MLANA*-specific gRNA, with or without the off-target A-to-G mismatch, each under control of the U6 promoter, were then inserted into the same plasmid. First, six Q5 High-Fidelity PCR reactions were performed on a plasmid expressing one copy of *MLANA*-specific gRNA under control of the U6 promoter. Each reaction was performed with a different pair of primers in order to create overlapping regions between each consecutive copy. The plasmid already containing *MLANA* and λN-$ADAR2_{DD}$(-NLS) was opened by restriction digestion with the enzyme ClaI (NEB, #R0197). The six PCR products were then inserted into the ClaI-digested plasmid in a single reaction with NEBuilder (NEB, #M5520AA). All cloning products were verified by control restriction digestion and Sanger sequencing. All primer sequences used for the PCR amplifications for plasmid construction are listed in Supplementary Table 1.

REFERENCES

1. C. Robert, A decade of immune-checkpoint inhibitors in cancer therapy. *Nat Commun* **11**, 3801 (2020).

2. C. Pilard, *et al.*, Cancer immunotherapy: it's time to better predict patients' response. *Br J Cancer* **125**, 927–938 (2021).

3. R. M. Samstein, *et al.*, Tumor mutational load predicts survival after immunotherapy across multiple cancer types. *Nat Genet* **51**, 202–206 (2019).

4. T. A. Chan, *et al.*, Development of tumor mutation burden as an immunotherapy biomarker: utility for the oncology clinic. *Annals of Oncology* **30**, 44–56 (2019).

5. J. Park, Y.-J. Chung, Identification of neoantigens derived from alternative splicing and RNA modification. *Genomics Inform* **17**, e23 (2019).

6. M. Zhang, *et al.*, RNA editing derived epitopes function as cancer antigens to elicit immune responses. *Nat Commun* **9**, 3919 (2018).

7. J. M. Gott, R. B. Emeson, Functions and mechanisms of RNA editing. *Annu. Rev. Genet.* **34**, 499–531 (2000).

8. K. Nishikura, Functions and Regulation of RNA Editing by ADAR Deaminases. *Annu. Rev. Biochem.* **79**, 321–349 (2010).

9. Y. A. Savva, L. E. Rieder, R. A. Reenan, The ADAR protein family. *Genome Biol* **13**, 252 (2012).

10. I. X. Wang, *et al.*, ADAR Regulates RNA Editing, Transcript Stability, and Gene Expression. *Cell Reports* **5**, 849–860 (2013).

11. V. Rayon-Estrada, *et al.*, Epitranscriptomic profiling across cell types reveals associations between APOBEC1-mediated RNA editing, gene expression outcomes, and cellular function. *Proc. Natl. Acad. Sci. U.S.A.* **114**, 13296–13301 (2017).

12. L. Zhang, C.-S. Yang, X. Varelas, S. Monti, Altered RNA editing in 3' UTR perturbs microRNA-mediated regulation of oncogenes and tumor-suppressors. *Sci Rep* **6**, 23226 (2016).

13. S. Ahmad, *et al.*, Breaching Self-Tolerance to Alu Duplex RNA Underlies MDA5-Mediated Inflammation. *Cell* **172**, 797-810.e13 (2018).

14. B. J. Liddicoat, A. M. Chalk, C. R. Walkley, ADAR1 , inosine and the immune sensing system: distinguishing self from non-self. *WIREs RNA* **7**, 157–172 (2016).

15. K. Pestal, *et al.*, Isoforms of RNA-Editing Enzyme ADAR1 Independently Control Nucleic Acid Sensor MDA5-Driven Autoimmunity and Multi-organ Development. *Immunity* **43**, 933–944 (2015).

16. H. Chung, *et al.*, Human ADAR1 Prevents Endogenous RNA from Triggering Translational Shutdown. *Cell* **172**, 811-824.e14 (2018).

17. N. Paz-Yaacov, *et al.*, Elevated RNA Editing Activity Is a Major Contributor to Transcriptomic Diversity in Tumors. *Cell Reports* **13**, 267–276 (2015).

18. X. Peng, *et al.*, A-to-I RNA Editing Contributes to Proteomic Diversity in Cancer. *Cancer Cell* **33**, 817-828.e7 (2018).

19. T. M. Woolf, J. M. Chase, D. T. Stinchcomb, Toward the therapeutic editing of mutated RNA sequences. *Proc. Natl. Acad. Sci. U.S.A.* **92**, 8298–8302 (1995).

20. T. Stafforst, M. F. Schneider, An RNA-Deaminase Conjugate Selectively Repairs Point Mutations. *Angew. Chem. Int. Ed.* **51**, 11166–11169 (2012).

21. M. F. Montiel-Gonzalez, I. Vallecillo-Viejo, G. A. Yudowski, J. J. C. Rosenthal, Correction of mutations within the cystic fibrosis transmembrane conductance regulator by site-directed RNA editing. *Proceedings of the National Academy of Sciences* **110**, 18285–18290 (2013).

22. B. Casati, D. Stamkopoulou, R. N. Tasakis, R. Pecori, "ADAR-Mediated RNA Editing and Its Therapeutic Potentials" in *Epitranscriptomics*, S. Jurga, J. Barciszewski, Eds. (Springer International Publishing, 2021), pp. 471–503.

23. D. B. T. Cox, *et al.*, RNA editing with CRISPR-Cas13. 1019–1027 (2017).

24. M. Fukuda, *et al.*, Construction of a guide-RNA for site-directed RNA mutagenesis utilising intracellular A-to-I RNA editing. *Sci Rep* **7**, 41478 (2017).

25. D. Katrekar, *et al.*, In vivo RNA editing of point mutations via RNA-guided adenosine deaminases. *Nat Methods* **16**, 239–242 (2019).

26. D. Katrekar, *et al.*, Efficient in vitro and in vivo RNA editing via recruitment of endogenous ADARs using circular guide RNAs. *Nat Biotechnol* (2022) https:/doi.org/10.1038/s41587-021-01171-4 (March 23, 2022).

27. T. Merkle, *et al.*, Precise RNA editing by recruiting endogenous ADARs with antisense oligonucleotides. *Nat Biotechnol* **37**, 133–138 (2019).

28. M. F. Montiel-González, I. C. Vallecillo-Viejo, J. J. C. Rosenthal, An efficient system for selectively altering genetic information within mRNAs. *Nucleic Acids Res*, gkw738 (2016).

29. L. Qu, *et al.*, Programmable RNA editing by recruiting endogenous ADAR using engineered RNAs. *Nat Biotechnol* **37**, 1059–1069 (2019).

30. P. Reautschnig, *et al.*, CLUSTER guide RNAs enable precise and efficient RNA editing with endogenous ADAR enzymes in vivo. *Nat Biotechnol* (2022) https:/doi.org/10.1038/s41587-021-01105-0 (March 23, 2022).

31. J. R. Sinnamon, *et al.*, Site-directed RNA repair of endogenous Mecp2 RNA in neurons. *Proc Natl Acad Sci USA* **114**, E9395–E9402 (2017).

32. J. R. Sinnamon, *et al.*, In Vivo Repair of a Protein Underlying a Neurological Disorder by Programmable RNA Editing. *Cell Reports* **32**, 107878 (2020).

33. P. Vogel, M. F. Schneider, J. Wettengel, T. Stafforst, Improving Site-Directed RNA Editing In Vitro and in Cell Culture by Chemical Modification of the GuideRNA. *Angew. Chem. Int. Ed.* **53**, 6267–6271 (2014).

34. P. Vogel, *et al.*, Efficient and precise editing of endogenous transcripts with SNAP-tagged ADARs. *Nat Methods* **15**, 535–538 (2018).

35. J. Wettengel, P. Reautschnig, S. Geisler, P. J. Kahle, T. Stafforst, Harnessing human ADAR2 for RNA repair – Recoding a PINK1 mutation rescues mitophagy. *Nucleic Acids Res*, gkw911 (2016).

36. Z. Yi, *et al.*, Engineered circular ADAR-recruiting RNAs increase the efficiency and fidelity of RNA editing in vitro and in vivo. *Nat Biotechnol* (2022) https:/doi.org/10.1038/s41587-021-01180-3 (March 7, 2022).

37. J. Galon, D. Bruni, Approaches to treat immune hot, altered and cold tumours with combination immunotherapies. *Nat Rev Drug Discov* **18**, 197–218 (2019).

38. L. A. Johnson, *et al.*, Gene Transfer of Tumor-Reactive TCR Confers Both High Avidity and Tumor Reactivity to Nonreactive Peripheral Blood Mononuclear Cells and Tumor-Infiltrating Lymphocytes. *The Journal of Immunology* **177**, 6548–6559 (2006).

39. P. Romero, *et al.*, Cytolytic T lymphocyte recognition of the immunodominant HLA-A*0201-restricted Melan-A/MART-1 antigenic peptide in melanoma. *The Journal of Immunology* **159**, 2366–2374 (1997).

40. M. Ayyoub, *et al.*, Activation of Human Melanoma Reactive CD8+ T Cells by Vaccination with an Immunogenic Peptide Analog Derived from Melan-A/Melanoma Antigen Recognized by T Cells-1. *Clinical Cancer Research* **9**, 669–677 (2003).

41. P. Romero, *et al.*, Antigenicity and immunogenicity of Melan-A/MART-1 derived peptides as targets for tumor reactive CTL in human melanoma. *Immunological Reviews* **188**, 81–96 (2002).

42. I. C. Vallecillo-Viejo, N. Liscovitch-Brauer, M. F. Montiel-Gonzalez, E. Eisenberg, J. J. C. Rosenthal, Abundant off-target edits from site-directed RNA editing can be reduced by nuclear localization of the editing enzyme. *RNA Biology* **15**, 104–114 (2018).

43. S. Chattopadhyay, J. Garcia-Mena, J. DeVito, K. Wolska, A. Das, Bipartite function of a small RNA hairpin in transcription antitermination in bacteriophage lambda. *Proc. Natl. Acad. Sci. U.S.A.* **92**, 4061–4065 (1995).

44. A. Kuttan, B. L. Bass, Mechanistic insights into editing-site specificity of ADARs. *Proc. Natl. Acad. Sci. U.S.A.* **109** (2012).

45. S. K. Wong, S. Sato, D. W. Lazinski, Substrate recognition by ADAR1 and ADAR2. *RNA* **7**, 846–858 (2001).

46. M. G. Kluesner, MultiEditR: The first tool for the detection and quantification of RNA editing from Sanger sequencing demonstrates comparable fidelity to RNA-seq. *Molecular Therapy*, 9 (2021).

47. M. F. Schneider, J. Wettengel, P. C. Hoffmann, T. Stafforst, Optimal guideRNAs for re-directing deaminase activity of hADAR1 and hADAR2 in trans. *Nucleic Acids Research* **42**, e87–e87 (2014).

48. Y. Iwai, *et al.*, Involvement of PD-L1 on tumor cells in the escape from host immune system and tumor immunotherapy by PD-L1 blockade. *Proceedings of the National Academy of Sciences* **99**, 12293–12297 (2002).

49. R. Cristescu, *et al.*, Tumor mutational burden predicts the efficacy of pembrolizumab monotherapy: a pan-tumor retrospective analysis of participants with advanced solid tumors. *J Immunother Cancer* **10**, e003091 (2022).

50. U. Sahin, *et al.*, Personalized RNA mutanome vaccines mobilize poly-specific therapeutic immunity against cancer. *Nature* **547**, 222–226 (2017).

51. M. Fukuda, K. Kurihara, Y. Tanaka, M. Deshimaru, A strategy for developing a hammerhead ribozyme for selective RNA cleavage depending on substitutional RNA editing. *RNA* **18**, 1735–1744 (2012).

52. S. Rauch, *et al.*, Programmable RNA-Guided RNA Effector Proteins Built from Human Parts. *Cell* **178**, 122-134.e12 (2019).

53. T. Tohama, M. Sakari, T. Tsukahara, Development of a Single Construct System for Site-Directed RNA Editing Using MS2-ADAR. *IJMS* **21**, 4943 (2020).

ACKNOWLEDGEMENTS

We thank the DKFZ Flow Cytometry Core Facility for their support with cell sorting experiments. This work was supported by Deutsche Forschungsgemeinschaft (DFG, German Research Foundation) - project number 439669440 TRR319 RMaP TP 04 awarded to F.N.P and the HI-TRON Kick-Start Seed Funding Program 2021 awarded to R.P.. V.P. and J.M.L. are supported by project funding for “Rapid Identification of Autoantigens in Autoimmune Disease” received from Janssen Pharmaceutical Companies of Johnson & Johnson.

AUTHOR CONTRIBUTIONS

Conceptualization, R.P., J.L. and F.N.P.; Methodology, B.C., V.P., R.P. and J.L.; Validation, B.C. and V.P.; Formal Analysis, B.C. and V.P.; Investigation, B.C. and V.P.; Writing – Original Draft, B.C. and V.P.; Writing – Review & Editing, B.C., V.P., R.P., J.L. and F.N.P.; Supervision, R.P., J.L. and F.N.P.; Project Administration, F.N.P.; Funding Acquisition, R.P., J.L. and F.N.P.

COMPETING INTERESTS

The DKFZ has filed a patent application regarding the described method (EP 23162121.0). B.C., R.P. and F.N.P. are inventors on the above-mentioned patent application.